Positive Feedback Regulation Between USP15 and ERK2 Promotes Cartilage Repair in Experimental Osteoarthritis

Wenjuan Wang
Shanghai Jiao Tong University School of Medicine
Yanhui Zhu
Shanghai Jiao Tong University School of Medicine
Zhenyu Sun
Shanghai Jiao Tong University School of Medicine
Chen Jin
Shanghai Jiao Tong University School of Medicine
Xiang Wang (wx20022005@outlook.com)
Shanghai Jiao Tong University School of Medicine https://orcid.org/0000-0001-8561-2724

Research

Keywords: Osteoarthritis, Adeno-associated virus, USP15, ERK2, TGF-β signaling pathway, Deubquitination, Positive feedback regulations

Posted Date: June 12th, 2020

DOI: https://doi.org/10.21203/rs.3.rs-34218/v1

Abstract

Background. The transforming growth factor-β (TGF-β) signaling pathway plays an essential role in maintaining homeostasis in joints affected by osteoarthritis (OA). Determine the specific relationship between non-SMAD and classical SMAD signaling pathways.

Methods. First,we found from human cartilage tissue specimens positive expressions of TGF-β1 and USP15between normal andosteoarthritiscartilage tissueby immunohistochemical.Then, overexpressing and knocking out USP15 or ERK2 followed bythe latest gene editing technology Crispr/Cas9 supported the studyinvitro.And we established rat knee OAmodelsthrough anterior cruciate ligament transection in combination with partial medial meniscectomy (ACLT+pMMx)after 8 weeksand conducted the corresponding Adeno-associated virus (AAV) intraarticular injections. Next, experimental data including immunohistochemical staining,HE/Safranin-O fast green staining,histological evidence analysis,relevant Osteoarthritis Research Society International (OARSI) scoresand expressions of molecules in cartilage anabolismindicated that the relationship betweenERK2 and USP15 throughTGF-β signaling pathway in vivo.Finally, we observed the specific mechanismof USP15 on ERK2 throughco-immunoprecipitation,deubiquitination assay, immunofluorescence and nuclear plasma separation.

Results. Here, we detected that ERK2 of non-SMAD signaling can maintain the cartilage phenotype by activating the TGF-β/Smad signaling pathway throughincreasing USP15 in vitro and in vivo. Most importantly, USP15 is required during this process and can form a complex with ERK2 to regulate ubiquitination of ERK2.Specifically,USP15, instead of USP15 C269S, deubiquitinates and activates ERK2, followed by translocation of phosphorylated ERK2 from the cytoplasm to the nucleus. Correspondingly, the level of phosphorylated ERK2 was increased by injecting AAV-mediated overexpressing USP15 into the rat OA model.

Conclusion. Taken together, our study revealed a positive feedback regulation between USP15 and ERK2, which plays a critical role in the interaction of SMAD and non-SMAD signaling pathways to promote cartilage repair in experimental OA.

Introduction

Osteoarthritis (OA), the most common chronic arthritis, is a complex and multifactorial disorder characterized by excessive degradation of articular cartilage that results in pain and disability [1, 2]. Disruption in the balance between anabolic and catabolic signaling pathways causes extracellular matrix damage to articular cartilage [3, 4]. Although many signaling mechanisms contribute to protective of cartilage, the stimulating molecular activities and pathways involved in inhibiting the development of OA remains imperfectly understood.

The transforming growth factor-β (TGF-β) signaling pathway plays an essential role in maintaining tissue homeostasis through anabolic signaling for cartilage growth and repair of cartilage [5]. TGF-β signaling is initiated by specific type I and II serine/threonine kinase receptors. The specific receptor-regulated (R)-

SMAD proteins, SMAD2 and SMAD3, which form a complex with SMAD4, a co-SMAD, are phosphorylated via the activated TGF-β type I receptor (TbRI). The SMAD complex is then efficiently transferred into the nucleus to regulate the transcription of target genes [6]. Furthermore, the TGF-β signaling pathway can be modified by ubiquitination to regulate downstream molecules [7]. Deubiquitinating enzymes (DUBs) can regulate target proteins by removing polyubiquitin chains. Recently, the ability of DUB USP15 to deubiquitinate and stabilize R-SMADs and TGF-β receptor I has gained great importance in our understanding of TGF-β signaling activity [8, 9], which attracted our attention in our current research.

Extracellular signal-regulated kinase (ERK), a member of the MAPK family, has been shown to be responsible for maintaining matrix anabolism and homeostasis of chondrocytes [10]. As described previously, ERK, part of the non-SMAD pathway of TGF-β signaling, modulates the TGF-β1/Smad pathway through enhancing Smad2/3 transcriptional activity [11, 12]. Of note, crosstalk mechanisms between ERK and SMAD pathways have been reported in many biological responses [13–16]. But the specific associations between ERK and SMAD pathways in OA have not yet been fully elucidated.

In the present study, we report that a positive feedback regulation between USP15 and ERK2 related to the SMAD and non-SMAD pathway could serve as an important quality control mechanism for prevention of cartilage matrix degradation in OA tissues.

Materials And Methods

Collection of human cartilage

Human articular cartilage was obtained from the femoral heads of female patients undergoing total hip replacement surgery at the Shanghai Ninth People's Hospital, Shanghai Jiao Tong University School of Medicine, following procedures approved by the Institutional Review Board. Cartilage from female patients with a fracture to the neck of the femur (n = 5, ages 65–95 years) was compared with cartilage from female patients with OA (n = 5, ages 36–87 years). OA was diagnosed according to the The American College of Rheumatology criteria for the classification [17]. The patients with fractures had no known history of joint disease, and their cartilage was free of lesions. These human cartilage tissues were used for subsequent histomorphological analysis by Safranin-O fast green staining and immunohistochemistry. All patients signed the informed consent.

Animals

Two-month-old male Norway rats (280–300 g; n = 42) were purchased from Shanghai SLAC Laboratory Animal Co. (Shanghai, China). All rats were randomly assigned to two models: sham surgery models (n = 14) and OA models (n = 28). All animal studies were conducted according to the guidelines of animal care and were approved by the Animal Care Committee of Shanghai Jiao Tong University.

Reagents

The following reagents were used: TGF-β1 (10 ng/ml; R&D Systems, Minneapolis, MN), MG132 (5 μM; Sigma-Aldrich, St. Louis, USA), Dulbecco's Modified Eagle's Medium (Gibco, Thermo Fisher Scientific, Waltham, USA), cycloheximide (100 μg/ml; Sigma-Aldrich), PD98059 (10 μM; Sigma-Aldrich).

In vivo rat OA model

Twenty four 2-month-old male Norway rats were anaesthetized by intraperitoneal injection with 3% pentobarbital sodium until cessation of all sensory reflexes. The right knees of rats were routinely disinfected with povidone iodine before surgery. The right knee joint was exposed by incision from the medial side of the patella, and the medial collateral ligament was removed to open the articular cavity. The rats then underwent anterior cruciate ligament transection in combination with partial medial meniscectomy (ACLT + pMMx) on the right knee as described previously [18, 19]. Finally, the incisions were sutured and ACLT + pMMx surgeries were induced after complete hemostasis was achieved. In the control group, the sham operations were performed on the model rats. After 8 weeks, OA models were successfully induced in rats that received the ACLT + pMMx surgeries.

Preparation of AAV vectors

Adeno-associated virus (AAV) serotype 2 vectors are AAV plasmids that can encode target genes and enhanced green fluorescent protein (EGFP) cDNA under control of the cytomegalovirus (CMV) enhancer. According to the previously reported method [20], serotype 2 of AAV (AAV-CMV-rUSP15-FLAG-T2A-EGFP and pAAV-U6-rERK2 [shRNA-1]-EGFP) packaged with two plasmids (pAAV-RC and pAAV-Helper) was obtained. The AAV knockdown sequence targeting ERK2 used was 5'- CTTCCAACCTCCTGCTGAA-3'.

AAV intraarticular injections

The two sub-control groups that received the sham surgeries were detailed as follows: (1) 7 rats without any injection. (2) 7 rats received a 30 μL intraarticular injection of pAAV-U6-rERK2 [shRNA-1]-EGFP (2.5×10^{10} vg) in the right knee joint.

The rat OA model groups that received the ACLT + pMMx surgeries were divided into four groups, as follows: (1) 14 OA model rats without any injection. (2) 7 OA model rats received a 30 μL intraarticular injection of pAAV-CMV-rUSP15-FLAG-T2A-EGFP (2.5×10^{10} vg) in the right knee joint. (3) 7 rats received a 30 μL injection of pAAV-CMV-rUSP15-FLAG-T2A-EGFP (2.5×10^{10} vg) followed by another 30 μL injection of pAAV-U6-rERK2 [shRNA-1]-EGFP (2.5×10^{10} vg).

Immunohistochemistry, HE/Safranin-O fast green staining and histology

Knee joints were fixed in 10% neutral buffered formalin for 3 d and decalcified in 10% EDTA solution at 4 °C for 3 months. Samples were dehydrated in ethanol, embedded in paraffin, and cut into coronal sections. Immunohistochemical results were detected with the following antibodies: Aggrecan (ab3778, Abcam), MMP13 (ab39012, Abcam), Col2a1 (ab34712, Abcam), TGF-β1 (ab92486, Abcam), USP15

(ab71713, Abcam), ERK2 (sc-1647, Santa Cruz Biotechnology, Dallas, USA), p-SMAD2 (ab188334, Abcam), p-ERK1/2 (4370S Cell Signaling Technology, Danvers, USA). Cartilage was stained with HE/Safranin-O fast green staining to observe general morphological changes. And then hyaline cartilage (HC) thickness were counted by at least three participants. Cartilage histological properties were assessed by the Osteoarthritis Research Society International (OARSI) scoring system as previously described [21, 22]. Double-blind histological evaluations of the cartilage lesions were performed in the whole analysis process.

Cell culture, transient transfections, and lentiviral infections

Primary chondrocytes were isolated from rat cartilage tissue as previously described [23]. Briefly, rats were euthanized by cervical dislocation and the hyaline cartilage of the femoral and tibial surfaces was removed with a scalpel. The pared hyaline cartilage was digested after cutting into pieces with hyaluronidase and collagenase II treatment. The isolated cells were cultured with Dulbecco's Modified Eagle Medium (DMEM) containing 10% fetal bovine serum (FBS) at 37 °C under a humidified atmosphere of 5% CO_2. To amplify the cultured cells, they were subcultured using 0.25% trypsin/EDTA. The isolated chondrocytes were identified by immunostaining for collagen II and Aggrecan.

ATDC5 cells (Riken Cell Bank, Tsukuba, Japan) were obtained and maintained in DMEM/F12 (1:1) (GIBCO) containing 5% FBS (HyClone, GE Healthcare Life Sciences, Chicago, USA), 100 U/mL penicillin, and 100 μg/mL streptomycin in a humidified incubator with 5% CO_2 at 37 °C. To induce chondrogenic differentiation, medium was supplemented with 10 μg/mL of insulin-transferrin-selenium (Thermo Fisher Scientific) after confluence and cells were cultured for 14 days. 293T cells (Riken Cell Bank, Tsukuba, Japan) were cultured in high glucose DMEM supplemented with 10% FBS and D-glutamate.

Transient transfections and lentiviral infections were performed as previously described [24]. HEK293T cells were transiently transfected with pLenti-CMV-mUSP15-FLAG-GFP-Puro, pLenti-CMV-mUSP15C269S-FLAG-GFP-Puro and pLenti-CMV-mERK2-HA-Puro. PLenti-CMV-mUSP15-FLAG-GFP-Puro, pLenti-CMV-mUSP15C269S-FLAG-GFP-Puro, pLenti-CMV-mERK2-HA-Puro, lentiCRISPRv2-USP15a, lentiCRISPRv2-USP15b, lentiCRISPRv2-ERK2a, lentiCRISPRv2-ERK2b and pLenti-CMV-Ub-His-Puro were co-transfected into HEK293T cells with the packaging plasmids pVSVg (AddGene 8454) and psPAX2 (AddGene 12260). The relevant CRISPR sequence were as follows: USP15-a-F: 5'-CACCG GGTATCTAGTAGATAGTCGG-3', USP15-a-R: 5'-AAAC CCGACTATCTACTAGATACCC-3', USP15-b-F: 5'-CACCG TGGCGACGCGCAGTCACTTA-3', USP15-b-R: 5'-AAAC TAAGTGACTGCGCGTCGCCAC-3', ERK2-a-F: 5'-CACCG CAGAGTACGTAGCCACACGT-3', ERK2-a-R: 5'-AAAC ACGTGTGGCTACGTACTCTGC-3', ERK2-b-F: 5'-CACCG GGATATACTTTAGCCCTCTC-3', ERK2-b-R: 5'-AAAC GAGAGGGCTAAAGTATATCCC-3'. ATDC5 cells were infected with the resulting stable lentiviral vectors.

Quantitative real-time RT-PCR

Total RNA was isolated from the ATDC5 cells or articular cartilage in rats by using Trizol (TaKaRa, Japan) according to the manufacturer's instructions. RNA was reverse-transcribed to cDNA with Reverse Transcription Kit (TaKaRa, Japan). Relative mRNA amount was quantified by Light Cycler 480 system (Roche, Switzerland) with SYBR Green I Kit (TaKaRa, Japan). The mouse primer sequences of the Col2a1, Col10a1, Sox9, Runx2 and GAPDH used were as follows: Col2a1: 5'-TACTGGAGTGACTGGTCCTAAG-3' (Forward) and 5'-AACACCTTTGGGACCATCTTTT-3' (Reverse), Col10a1: 5'-GAATTTCTGTGCCAGGAAAACC-3' (Forward) and 5'-TTTTCACCTCTTCTTCCCACTC-3' (Reverse), Sox9: 5'-GAGTTTGACCAATACTTGCCAC-3' (Forward) and 5'-GTAACTGCCAGTGTAGGTGAC-3' (Reverse), Runx2: 5'-CCTTCAAGGTTGTAGCCCTC-3' (Forward) and 5'-GGAGTAGTTCTCATCATTCCCG-3' (Reverse), GAPDH: 5'-CACTCTTCCACCTTCGATGC-3' (Forward) and 5'-TCTTGCTCAGTGTCCTTGCT-3' (Reverse). The rat primer sequences of the Col2a1, Aggrecan, Sox9 and GAPDH used were as follows: Col2a1: 5'-GGAGCAGCAAGAGCAAGGAGAAG-3' (Forward) and 5'-GGAGCCCTCAGTGGACAGTAGAC-3' (Reverse), Aggrecan: 5'-GCTACGACGCCATCTGCTACAC-3' (Forward) and 5'- ATGTCCTCTTCACCACCCACTCC-3' (Reverse), Sox9: 5'-TGGCAGAGGGTGGCAGACAG-3' (Forward) and 5'-CGTTGGGCGGCAGGTATTGG-3' (Reverse), GAPDH: 5'- ATGGTGAAGGTCGGTGTGAA-3' (Forward) and 5'-CACCACCCTGTTGCTGTAGC-3' (Reverse). Relative amounts of mRNA were standardized and calculated as previously described [25, 26].

Western blotting

Cell extracts were subjected to SDS-PAGE in 10% polyacrylamide gels, followed by blotting onto polyvinylidene difluoride membranes (Millipore, Bedford, USA). Primary antibodies included p-ERK1/2, FLAG, Ubiquitination, GAPDH (Cell Signaling Technology,); ERK1, ERK2, HA, His (Santa Cruz Biotechnology); USP15, p-SMAD2, SMAD2, SMAD4 (Abcam). Corresponding species-specific secondary antibodies (anti-rabbit IgG HRP, anti-mouse IgG HRP) were used. GAPDH was used to normalize the results adjusting for control variations between individual experiments. The results were detected by a Western Chemiluminescent HRP Substrate kit (Millipore, Burlington, USA) and imaged using the FluorChem M system (Protein Simple, San Jose, USA).

Co-immunoprecipitation and deubiquitination assay

Monolayer cultured cells were added to ice cold RIPA buffer and centrifuged at 10,000 *g* for 10 min at 4 °C. The supernatant was transferred to a fresh 1.5 mL conical centrifuge tube on ice with 5 μL of indicated antibodies and 20 μL of resuspended volume of Protein A/G PLUS-Agarose (Santa Cruz Biotechnology), and then incubated overnight at 4 °C on a rocker platform. Co-immunoprecipitates were collected and the supernatant discarded. The pellet was washed 4 × with 1.0 mL RIPA buffer. After the final wash, samples were boiled for 10 min and analyzed by Western blotting. To detect ERK2 deubiquitination, transient transfections and lentiviral stable infections were performed before co-immunoprecipitation.

Immunofluorescence staining

Immunofluorescence staining was performed as previously described [27, 28]. In brief, cells were fixed with 4% formaldehyde and incubated with USP15, ERK2, p-ERK1/2, HA, FLAG, Aggrecan, Col2a1 and Col10a1 antibodies. Immunofluorescence staining results were detected with the following antibodies: Col2a1 (ab34712, Abcam), Aggrecan (ab3778, Abcam), Col10a1 (ab49945, Abcam) and other antibodies were described above. Samples were then treated by a secondary antibody. Nuclear DNA was visualized by DAPI staining and viewed under an immunofluorescence confocal microscope (NIKON Eclipse Ti, Japan).

Results

USP15 is negatively correlated with cartilage destruction in human cartilage of OA

First of all, we performed relevant histomorphological analysis of each human sample by Safranin-O staining in our study. The results showed that compared with normal human cartilage tissue, the cartilage surface of human OA cartilage tissue was rough, uneven and severely damaged. Subsequently, the Safranin-O color of the hyaline cartilage became lighter, the thickness decreased, and its OARSI score statistically significant increased (Fig. 1A, C).

From the statistics, OA human cartilage revealed weaker Aggrecan and stronger MMP13 immunostaining than was observed in the normal human cartilage (Fig. 1B, C). Relative to the normal human cartilage, immunohistochemical staining results showed that levels of TGF-β1 and USP15 decreased in human cartilage of OA (Fig. 1B, C). These results inspired us to further study the role of USP15 in the SMAD pathway of OA in the following experiments.

USP15 is conducive to cartilage repair in vitro and in vivo

We assessed the mechanism of USP15 regulating the TGF-β signaling pathway. In ADTC5 cells, ITS induction solution was added to continuously induce cartilage phenotype, and PCR detection of cartilage phenotype related marker molecules was performed at 7, 14 and 21 days respectively. It was confirmed that the expression levels of Col2a1 and Sox9 would peak at 14 days. Col10a1 peaked after 21 days of induction, and Runx2 decreased gradually after 7 days of induction. According to the results of this experiment and relevant literature reports[29, 30], we set 14 days as the optimal cartilage induction time (Fig. 2A). All the subsequent experiments required ATDC5 cells that had been induced. Overexpression of USP15, rather than USP15 mutant USP15 C269S (enzymatically inactive USP15), led to an increase of phosphorylated SMAD2 (p-SMAD2) (Fig. 2B). In contrast, endogenous USP15 knocked out by Crispr/Cas9 in untreated and TGF-β1-treated ATDC5 cells decreased the level of p-SMAD2 instead of total expression of SMAD2 and SMAD4 (Fig. 2C). Compared with the role of Crispr USP15a, Crispr USP15b has a more obvious influence on decreasing p-SMAD2, so we selected the sequence of Crispr USP15b for subsequent experiments. Immunofluorescence staining in ATDC5 cells demonstrated that USP15 could increase molecules involved in cartilage anabolic metabolism Col2a1 and Aggrecan concentrations, and the Col10a1 of inhibiting the formation of cartilage decreased (Fig. 2D,E).

To further determine whether USP15 has an inhibitory effect on chondrocyte destruction, we injected rat OA models with AAV-mediated USP15 overexpression in situ. Immunostaining results demonstrated there were higher levels of USP15, p-SMAD2, Col2a1 and Aggrecan in the AAV-mediated USP15 overexpression groups than the control groups of the OA models (Fig. 2F, I). Histological analysis was performed in the HE/Safranin-O fast green staining (Fig. 2G-I). Compared to the control group, the stained Safranin-O color of the cartilage in the USP15 overexpression group was deeper and the articular plane was repaired (Fig. 2H). The thickness of hyaline cartilage was measured and OARSI was scored for each group according to the staining results. It can be concluded that USP15 overexpression can significantly increase the thickness of hyaline cartilage, and its OARSI score is much lower than that of the control group (Fig. 2I).To further verify the protective role of USP15 in cartilage, we detected some promoting cartilage anabolic molecules by real-time quantitative PCR in rat cartilage tissue, and the results showed that the overexpression of USP15 increased the expression of Col2a1, Aggrecan and Sox9 (Fig. 2J).

ERK2 can maintain the cartilage phenotype by regulating the TGF-β signaling pathway through USP15

To determine whether ERK2 can regulate USP15 to influence the TGF-β signaling pathway, we transfected lentivirals to overexpress and knock out ERK2 in ATDC5 cells. When ERK2 was overexpressed, the expression of USP15 increased in untreated and TGF-β1-treated ATDC5 cells. Subsequently, p-SMAD2 was evidently activated in the TGF-β signaling pathway (Fig. 3A). These results also indicated that the levels of USP15 and p-SMAD2 were suppressed with knocked out of ERK2 (Fig. 3C). After treating ATDC5 cells with the extracellular-signal-regulated kinase (ERK)-pathway inhibitor PD98059, the level of p-SMAD2 decreased despite overexpression of ERK2 (Fig. 3B). Furthermore, total expression of SMAD2 and SMAD4 were unchanged after undergoing these treatments (Fig. 3A-C). Finally, immunofluorescence staining results in ATDC5 cell revealed that ERK2 can also maintain the cartilage phenotype and inhibit the destruction factor of cartilage formation by statistic analysis of data (Fig. 3D,E).

Notably, it was reported that ERK2 is crucial for the activity of R-Smads [(31)]. We also observed that AAV-mediated ERK2 knockdown reduced the levels of USP15, p-SMAD2, Col2a1 and Aggrecan in rat sham surgery model knee joints (Fig. 3F). Under the influence of ERK2 knockdown, the HE/Safranin-O staining thickness of the cartilage in OA was significantly reduced and the articular surface became rough (Fig. 3G-I). In the sham surgery models, we then performed real-time quantitative PCR in the control groups and the AAV-mediated ERK2 knockdown groups of rat cartilage to detect some of the molecules that promote anabolic metabolism of cartilage, and the results showed that the knockdown of ERK2 reduced the expression of Col2a1, Aggrecan and Sox9 (Fig. 3J). In vitro and in vivo experiments showed that ERK2 had a certain inhibitory effect on cartilage degradation, and it could enhance TGF-β signaling pathway by upregulation of the expression of USP15, thus affecting cartilage repair.

ERK2 requires USP15 to influence the TGF-β signaling pathway

We transfected lentivirus ERK2 overexpression and USP15 knockout at the same time in ATDC5 cells in vitro. The levels of p-SMAD2 declined with decreasing USP15 despite overexpression of ERK2 (Fig. 4A).

Immunofluorescence staining results further revealed that compare to ERK2, USP15 has more influence on maintenance of cartilage phenotype such as increasing the expressing of Col2a1 and Aggrecan except for the expressing of Col10a1 (Fig. 4B,C). Taken together, these results confirm that USP15 is required for ERK2 to influence the TGF-β signaling pathway.

To further evaluate the role of USP15 in the TGF-β signaling pathway, we used injections of AAV-mediated USP15 overexpression and ERK2 knockdown simultaneously in the OA models rat articular cavities. According to the results of immunohistochemistry, when overexpressing USP15 and knocking down ERK2 at the same time, the expression of p-SMAD2, Col2a1 and Aggrecan in the cartilage of the knee joint of rats was relatively increased, indicating that the TGF-β signaling pathway was strengthened (Fig. 4D). In this rescue case, the HE/Safranin-O staining of the cartilage increased, and we can see that the increasing thickness of the hyaline cartilage, the smoother articular surface, and the decreasing loss of chondrocytes (Fig. 4E, F). We then performed a quantitative analysis of hyaline cartilage thickness and OARSI score to further confirm our observation (Fig. 4G). Next the real-time quantitative PCR results showed that when overexpression of USP15 was combined with the knocking down of ERK2, the expression of Col2a1, Aggrecan and Sox9 quantity increased to the inhibition of the destroyed cartilage (Fig. 4H). In the in vivo experiments of rats, when the overexpression of USP15 was combined with the knocking down of ERK2 in the OA model, its effect was finally to inhibit the injury of the knee cartilage of rats. Therefore, the TGF-β signaling pathway was mainly influenced by the trend of USP15, and in vitro and in vivo experiments showed that USP15 played a full and necessary role in ERK2's transduction of TGF-β signaling pathway to the downstream cartilage phenotype.

USP15 can form a complex with ERK2

We investigated the underlying relationship between USP15 and ERK2 by co-immunoprecipitation assays. Indeed, endogenous USP15 can form a complex with endogenous ERK2 in rat articular chondrocytes (Fig. 5A). The binding interaction was further found between ectopically overexpressed Flag-tagged USP15 and HA-tagged ERK2 by co-immunoprecipitation in 293T cells (Fig. 5B).

To observe the USP15 binding region involved in ERK2 interaction, we used three truncated proteins from USP15 to co-immunoprecipitate with ERK2 (Fig. 5C). The results demonstrated that the N terminus domain of USP15 was bound to ERK2 (Fig. 4C), which was further exhibited by immunofluorescence staining results revealing the colocalization of exogenous ERK2 and USP15 or its mutant in ATDC5 cells (Fig. 5D).

USP15 regulates ubiquitination of ERK2.

Since USP15 can interact with ERK2, we hypothesized that USP15 deubiquitinates ERK2. First, we co-expressed HA-tagged ERK2 along with His-tagged ubiquitination and found that ERK2 could be ubiquitinated in ATDC5 cells (Fig. 6A). Next, HA-tagged ERK2 and His-tagged Ubiquitination expression vectors were co-expressed with Flag-tagged USP15 wild-type or USP15C269S in ATDC5 cells (Fig. 6B). A loss of ubiquitination of ERK2 was detected by overexpression of USP15 wild-type but not the

catalytically inactive USP15 mutant. Conversely, USP15 depletion markedly enhanced the incorporation of ubiquitin into ERK2 (Fig. 6C).

We therefore investigated whether USP15 affects the stability of ERK2. Surprisingly, the total amount of ERK2 was unchanged by treatment with the proteasome inhibitor MG132 (Fig. 6D). When treated with cycloheximide, overexpressed Flag-tagged USP15 could not protect the ERK2 half-life (Fig. 5E). Additionally, knocking out USP15 expression could not influence the ERK2 concentration (Fig. 6D). However, these data indicated that MG132 induced ERK2 activation and active USP15 could increase phosphorylated ERK2 (p-ERK2) stability and half-life (Fig. 6D,E).

USP15 changes the location of ERK2 and stimulates the p-ERK2 level

As previously mentioned, USP15 failed to affect the expression of ERK2. However, we evaluated the subcellular distribution of endogenous ERK2 and p-ERK2 by treatments with overexpressed Flag-tagged USP15 instead of USP15C269S. According to the results of isolating the nuclear and cytoplasmic proteins or immunofluorescence microscopy, overexpressing USP15 instead of its mutant could increase the cytoplasmic signal of endogenous ERK2 and decrease the nuclear amount of endogenous ERK2 (Fig. 7A, B). Importantly, treatment with overexpressed Flag-tagged USP15 activated nuclear p-ERK2 validated by immunofluorescence measurements (Fig. 7C). Furthermore, through the experimental study of immunohistochemistry, we also verified once again that the overexpressed USP15 can increase the phosphorylation of ERK2 in the OA models comparing the control groups and the AAV-mediated USP15 overexpression groups (Fig. 7D, E).

Discussion

OA is the most common type of arthritis with inflammatory disease in the synovial joints [32, 33]. It is characterized by gradual degeneration of articular cartilage and changes in the structure and function of the entire joint [34, 35]. In recent years, it has been reported that the canonical SMAD signaling of the TGF-β signaling pathway contribute significantly to cartilage maintenance and repair. To our knowledge, the intricate mechanisms between SMAD and non-SMAD pathways in OA tissues were not yet fully characterized [36–38]. In our study, we further investigated specific regulation between USP15 and ERK2 related to the SMAD and non-SMAD pathway to provide an innovative direction to explore the occurrence and treatment of OA.

In order to investigate the expression of TGF-β signaling pathway related molecules in human cartilage, we first collected normal and osteoarthritic human cartilage following hip replacement. Then, we found that the destruction of the hip joint cartilage with OA was quite serious. The surface of the cartilage was rough with cracks. The thickness of hyaline cartilage was significantly reduced compared with the normal sample and the OARSI score was also significantly increased, which were similar to previous reports [39]. Secondly, as indicated by the immunohistochemical results, the more severe the cartilage surface destruction, the lower the expression levels of Aggrecan, TGF-β1 and USP15, and on the contrary, the

higher the expression levels of MMP13. This result suggests that we need to pay more attention to the signaling activities of TGF-β signaling pathway related USP15 in our study.

From the beginning of the vitro experiment, we found that endogenous USP15 could bind to ERK1 in rat chondrocytes through co-immunoprecipitation (Supplement Fig. 1A). Therefore, we started to verify the relationship between them. But the western blot results showed that the expression level of USP15 was unchanged when ERK1 knocked down in ATDC5 cells (Supplement Fig. 1B). Then, we observed that the amount of USP15 was constant by knocking out or overexpressing ERK1 in ATDC5 cells (Supplement Fig. 1C, D). Definitely, we chose to study the relationship between USP15 and ERK2 deeply in the follow-up experiments.

It was reported that USP15 could be regarded as a responding marker of the TGF-β signaling pathway [(40)]. Consistent with the in vivo measurement indications of AAV-mediated USP15 overexpression, we observed that USP15 stimulated the TGF-β signaling pathway such as p-SMAD2, p-ERK2 and caused chondrocyte remodeling with increasing Col2a1, Aggrecan, and Sox9 levels. Histological assessments further revealed that USP15 was beneficial to developments of cartilage repair. Our findings with ATDC5 cells further demonstrated that only activated USP15, and not USP15C269S, is important for enhancing SMAD signaling responses.

ERK2 of non-SMAD pathways is known to regulate the TGF-β signaling pathway through SMADs [(41)]. As expected, in vitro data suggested that ERK2 overexpression can increase the level of p-ERK2 and activate p-SMAD2 by enhancing USP15 concentrations. Even though ERK2 was overexpressed, the amount of p-SMAD2 was still decreased with p-ERK2 inhibited. This result demostrated that overexpressed ERK2 also can stimulate p-SMAD2 directly through increasing p-ERK2. Similarly, knocking down ERK2 in the sham surgery models could weaken the TGF-β signaling pathway followed by cartilage damage. Hence, elevating ERK2 levels suppressed cartilage damage through the TGF-β signaling pathway. To address whether USP15 is required between ERK2 and p-SMAD2, we performed rescue experiments in both rat models and ATDC5 cells. Taken as a whole, although ERK2 was knocked down, p-SMAD2 expression was increased due to upregulation of USP15 expression. Eventually, the expression levels of molecules such as Col2a1,Aggrecan and Sox9 that promoting cartilage repair elevated.

Co-immunocoprecipitation assays in our current studies showed that USP15 could bind to ERK2. Because USP15 is an indispensable deubiquitinating enzyme for the TGF-β signaling pathway, we speculated that USP15 could deubiquitinate ERK2. To verify this deubiquitination modification, we determined that ERK2 could be deubiquitinated. In agreement with our prediction, we analyzed the specific deubiquitination effects of USP15 towards ERK2. If USP15 was knocked out, ERK2 would undergo more ubiquitination modifications. The most common role in ubiquitination is protein degradation [(42–44)] Surprisingly, even though USP15 could deubiquitinate ERK2, the degradation of endogenous ERK2 was not changed by USP15. Next, we identified that the total ERK2 levels were unchanged when treated with the proteasome inhibitor MG132. Interestingly, overexpressed USP15 could stabilize p-ERK2 with or without MG132 treatment. From the half-life experiment with cycloheximide, we observed that overexpressed Flag-tagged

USP15 could prolong the half-life of p-ERK2. To some extent, the degradation of p-ERK2 was prevented by USP15. Otherwise, USP15 instead of USP15C269S, can cause an increase in the distribution of ERK2 in the cytoplasm and a decrease in the distribution of ERK2 in the nucleus. Then, USP15 activates ERK2, and p-ERK2 from the cytoplasm is translocated to the nucleus. In vivo, the level of p-ERK2 increased by AAV-mediated upregulated USP15 in rat OA model knee joints. Finally, a working model for positive feedback regulation between USP15 and ERK2 that enhanced the intracellular responses to the TGF-β signaling pathway, which may present potential therapeutic value for OA treatment was described (Fig. 8).

The limitations of this study included that there were only rat OA models instead of human clinical samples to explore deeper mechanisms in the further study. What's more, primary chondrocytes isolated from rat cartilage tissue were replaced by ATDC5 cells in the part of vitro study because of the difficult lentiviral infections in them.

In conclusion, the present study suggests that positive feedback regulation between USP15 and ERK2 plays a critical role in the interactions of SMAD and non-SMAD signaling pathways. However, the cascade of interconnected responses provides new insights into the pathogenesis of OA. Additionally, the positive feedback loop should be considered a powerful therapeutic target for the clinical treatment for OA.

Declarations

Ethics approval and consent to participate:

The human and animal study were reviewed and approved by Animal CareCommittee of Shanghai Jiao Tong University.

Consent for publication:

All authors were consent for publication.

Availability of data and material:

All datasets generated for this study are included in the article/supplementary material.

Competing interests:

All authors state that they have no conflicts of interest.

Funding:

The research was supported by Natural Science Foundation of Shanghai (17ZR1416600).

Authors' Contributions:

WW, CJ and XW designed research; CJ and XW analyzed data; WW, YZ and ZS performed research; WW, YZ and ZS wrote the paper; WW and YZ contributed new reagents or analytic tools; WW and ZS developed software necessary to perform and record experiments.

Acknowledgements:

The authors acknowledge all authors who contributed tothis manuscript.

References

1. Glyn-Jones S, Palmer AJ, Agricola R, Price AJ, Vincent TL, Weinans H, et al. Osteoarthritis Lancet Jul. 2015;25(9991):376–87. 386(. Epub 2015/03/10.
2. Roos EM, Arden NK. Strategies for the prevention of knee osteoarthritis. Nat Rev Rheumatol Feb. 2016;12(2):92–101. Epub 2015/10/07.
3. Guilak F. Biomechanical factors in osteoarthritis. Best Pract Res Clin Rheumatol Dec. 2011;25(6):815–23. Epub 2012/01/24.
4. Schroeppel JP, Crist JD, Anderson HC, Wang J. Molecular regulation of articular chondrocyte function and its significance in osteoarthritis. Histol Histopathol Mar. 2011;26(3):377–94. Epub 2011/01/07.
5. Chen CG, Thuillier D, Chin EN, Alliston T. Chondrocyte-intrinsic Smad3 represses Runx2-inducible matrix metalloproteinase 13 expression to maintain articular cartilage and prevent osteoarthritis. Arthritis Rheum Oct. 2012;64(10):3278–89. Epub 2012/06/08.
6. Xi Q, Wang Z, Zaromytidou AI, Zhang XH, Chow-Tsang LF, Liu JX, et al. A poised chromatin platform for TGF-beta access to master regulators. Cell Dec. 2011;23(7):1511–24. 147(. Epub 2011/12/27.
7. Zhang L, Zhou F, Garcia de Vinuesa A, de Kruijf EM, Mesker WE, Hui L, et al. TRAF4 promotes TGF-beta receptor signaling and drives breast cancer metastasis. Mol Cell Sep. 2013;12(5):559–72. 51(. Epub 2013/08/27.
8. Inui M, Manfrin A, Mamidi A, Martello G, Morsut L, Soligo S, et al. USP15 is a deubiquitylating enzyme for receptor-activated SMADs. Nat Cell Biol Sep. 2011;25(11):1368–75. 13(. Epub 2011/09/29.
9. Eichhorn PJ, Rodon L, Gonzalez-Junca A, Dirac A, Gili M, Martinez-Saez E, et al. USP15 stabilizes TGF-beta receptor I and promotes oncogenesis through the activation of TGF-beta signaling in glioblastoma. Nat Med Feb. 2012;19(3):429–35. 18(. Epub 2012/02/22.
10. Wei JL, Fu W, Ding YJ, Hettinghouse A, Lendhey M, Schwarzkopf R, et al. Progranulin derivative Atsttrin protects against early osteoarthritis in mouse and rat models. Arthritis Res Ther Dec. 2017;19(1):280. 19(. Epub 2017/12/21.
11. Yoon JH, Sudo K, Kuroda M, Kato M, Lee IK, Han JS, et al. Phosphorylation status determines the opposing functions of Smad2/Smad3 as STAT3 cofactors in TH17 differentiation. Nat Commun Jul. 2015;21:6:7600. Epub 2015/07/22.

12. Zhang YE. Non-Smad Signaling Pathways of the TGF-beta Family. Cold Spring Harb Perspect Biol. Feb 1 2017;9(2). Epub 2016/11/20.
13. Zeng H, Yang Z, Xu N, Liu B, Fu Z, Lian C, et al. Connective tissue growth factor promotes temozolomide resistance in glioblastoma through TGF-beta1-dependent activation of Smad/ERK signaling. Cell Death Dis Jun. 2017;15(6):e2885. 8(. Epub 2017/06/16.
14. Fuentealba LC, Eivers E, Ikeda A, Hurtado C, Kuroda H, Pera EM, et al. Integrating patterning signals: Wnt/GSK3 regulates the duration of the BMP/Smad1 signal. Cell Nov. 2007;30(5):980–93. 131(. Epub 2007/11/30.
15. Derynck R, Zhang YE. Smad-dependent and Smad-independent pathways in TGF-beta family signalling. Nature Oct. 2003;9(6958):577–84. 425(. Epub 2003/10/10.
16. Hu X, Ji X, Yang M, Fan S, Wang J, Lu M, et al. Cdc42 Is Essential for Both Articular Cartilage Degeneration and Subchondral Bone Deterioration in Experimental Osteoarthritis. J Bone Miner Res May. 2018;33(5):945–58. Epub 2018/01/10.
17. Altman R, Alarcon G, Appelrouth D, Bloch D, Borenstein D, Brandt K, et al. The American College of Rheumatology criteria for the classification and reporting of osteoarthritis of the hip. Arthritis Rheum May. 1991;34(5):505–14. Epub 1991/05/01.
18. Deshmukh V, Hu H, Barroga C, Bossard C, Kc S, Dellamary L, et al. A small-molecule inhibitor of the Wnt pathway (SM04690) as a potential disease modifying agent for the treatment of osteoarthritis of the knee. Osteoarthritis Cartilage Jan. 2018;26(1):18–27. Epub 2017/09/11.
19. Hamilton CB, Pest MA, Pitelka V, Ratneswaran A, Beier F, Chesworth BM. Weight-bearing asymmetry and vertical activity differences in a rat model of post-traumatic knee osteoarthritis. Osteoarthritis Cartilage Jul. 2015;23(7):1178–85. Epub 2015/03/17.
20. Payne KA, Lee HH, Haleem AM, Martins C, Yuan Z, Qiao C, et al. Single intra-articular injection of adeno-associated virus results in stable and controllable in vivo transgene expression in normal rat knees. Osteoarthritis Cartilage Aug. 2011;19(8):1058–65. Epub 2011/05/17.
21. Aigner T, Cook JL, Gerwin N, Glasson SS, Laverty S, Little CB, et al. Histopathology atlas of animal model systems - overview of guiding principles. Osteoarthritis Cartilage Oct. 2010;18(Suppl 3):2–6. Epub 2010/10/01.
22. Gerwin N, Bendele AM, Glasson S, Carlson CS. The OARSI histopathology initiative - recommendations for histological assessments of osteoarthritis in the rat. Osteoarthritis Cartilage Oct. 2010;18(Suppl 3):24–34. Epub 2010/10/01.
23. Filip A, Pinzano A, Bianchi A, Feve B, Jalkanen S, Gillet P, et al. Expression of the semicarbazide-sensitive amine oxidase in articular cartilage: its role in terminal differentiation of chondrocytes in rat and human. Osteoarthritis Cartilage Jul. 2016;24(7):1223–34. Epub 2016/02/07.
24. Zhang Q, Xiao M, Gu S, Xu Y, Liu T, Li H, et al. ALK phosphorylates SMAD4 on tyrosine to disable TGF-beta tumour suppressor functions. Nat Cell Biol Feb. 2019;21(2):179–89. Epub 2019/01/22.
25. Su X, Lu L, Li Y, Zhen C, Hu G, Jiang K, et al. Reference gene selection for quantitative real-time PCR (qRT-PCR) expression analysis in Galium aparine L. PLoS One. 2020;15(2):e0226668. Epub

2020/02/06.

26. Bai B, Ren J, Bai F, Hao L. Selection and validation of reference genes for gene expression studies in Pseudomonas brassicacearum GS20 using real-time quantitative reverse transcription PCR. PLoS One. 2020;15(1):e0227927. Epub 2020/01/28.
27. Liu H, Zhang H, Wang X, Tian Q, Hu Z, Peng C, et al. The Deubiquitylating Enzyme USP4 Cooperates with CtIP in DNA Double-Strand Break End Resection. Cell Rep Oct. 2015;6(1):93–107. 13(. Epub 2015/09/22.
28. Zhang L, Zhou F, Drabsch Y, Gao R, Snaar-Jagalska BE, Mickanin C, et al. USP4 is regulated by AKT phosphorylation and directly deubiquitylates TGF-beta type I receptor. Nat Cell Biol Jun. 2012;17(7):717–26. 14(. Epub 2012/06/19.
29. Ma Y, Liu Y, Ma Y, Jiang N, Wang L, Wang B, et al. Mangiferin Relieves Lipopolysaccharide-Induced Injury by Up-Regulating miR-181a via Targeting PTEN in ATDC5 Cells. Front Pharmacol. 2020;11:137. Epub 2020/03/27.
30. Li D, Li G, Chen Y, Li Y, Zhang J, Gao D, et al. Astragaloside IV protects ATDC5 cells from lipopolysaccharide-caused damage through regulating miR-203/MyD88. Pharm Biol Dec. 2020;58(1):89–97. Epub 2020/01/08.
31. Lu L, Wang J, Zhang F, Chai Y, Brand D, Wang X, et al. Role of SMAD and non-SMAD signals in the development of Th17 and regulatory T cells. J Immunol Apr. 2010;15(8):4295–306. 184(. Epub 2010/03/23.
32. Chu L, Liu X, He Z, Han X, Yan M, Qu X, et al. Articular Cartilage Degradation and Aberrant Subchondral Bone Remodeling in Patients with Osteoarthritis and Osteoporosis. J Bone Miner Res Mar. 2020;35(3):505–15. Epub 2019/11/07.
33. Zhang M, Yang H, Wan X, Lu L, Zhang J, Zhang H, et al. Prevention of Injury-Induced Osteoarthritis in Rodent Temporomandibular Joint by Targeting Chondrocyte CaSR. J Bone Miner Res Apr. 2019;34(4):726–38. Epub 2018/11/30.
34. Richard D, Liu Z, Cao J, Kiapour AM, Willen J, Yarlagadda S, et al. Evolutionary Selection and Constraint on Human Knee Chondrocyte Regulation Impacts Osteoarthritis Risk. Cell Apr. 2020;16(2):362–81. 181(e28. Epub 2020/03/30.
35. Mazur CM, Woo JJ, Yee CS, Fields AJ, Acevedo C, Bailey KN, et al. Osteocyte dysfunction promotes osteoarthritis through MMP13-dependent suppression of subchondral bone homeostasis. Bone Res. 2019;7:34. Epub 2019/11/09.
36. Zhang T, Wen F, Wu Y, Goh GS, Ge Z, Tan LP, et al. Cross-talk between TGF-beta/SMAD and integrin signaling pathways in regulating hypertrophy of mesenchymal stem cell chondrogenesis under deferral dynamic compression. Biomaterials Jan. 2015;38:72–85. Epub 2014/12/03.
37. Rostam MA, Kamato D, Piva TJ, Zheng W, Little PJ, Osman N. The role of specific Smad linker region phosphorylation in TGF-beta mediated expression of glycosaminoglycan synthesizing enzymes in vascular smooth muscle. Cell Signal Aug. 2016;28(8):956–66. Epub 2016/05/08.

38. Beyer C, Zenzmaier C, Palumbo-Zerr K, Mancuso R, Distler A, Dees C, et al. Stimulation of the soluble guanylate cyclase (sGC) inhibits fibrosis by blocking non-canonical TGFbeta signalling. Ann Rheum Dis Jul. 2015;74(7):1408–16. Epub 2014/02/26.
39. Kang X, Qian Z, Liu J, Feng D, Li H, Zhang Z, et al. Neuropeptide Y Acts Directly on Cartilage Homeostasis and Exacerbates Progression of Osteoarthritis Through NPY2R. J Bone Miner Res. Feb 26 2020. Epub 2020/02/27.
40. Liu WT, Huang KY, Lu MC, Huang HL, Chen CY, Cheng YL, et al. TGF-beta upregulates the translation of USP15 via the PI3K/AKT pathway to promote p53 stability. Oncogene May. 2017;11(19):2715–23. 36(. Epub 2016/11/29.
41. Zhang X, Arnott JA, Rehman S, Delong WG Jr, Sanjay A, Safadi FF, et al. Src is a major signaling component for CTGF induction by TGF-beta1 in osteoblasts. J Cell Physiol Sep. 2010;224(3):691–701. Epub 2010/05/01.
42. Wang L, Wu J, Li J, Yang H, Tang T, Liang H, et al. Host-mediated ubiquitination of a mycobacterial protein suppresses immunity. Nature Jan. 2020;577(7792):682–8. Epub 2020/01/17.
43. Gan N, Zhen X, Liu Y, Xu X, He C, Qiu J, et al. Regulation of phosphoribosyl ubiquitination by a calmodulin-dependent glutamylase. Nature Aug. 2019;572(7769):387–91. Epub 2019/07/23.
44. Worden EJ, Hoffmann NA, Hicks CW, Wolberger C. Mechanism of Cross-talk between H2B Ubiquitination and H3 Methylation by Dot1L. Cell Mar. 2019;7(6):1490–501. 176(e12. Epub 2019/02/16.

Figures

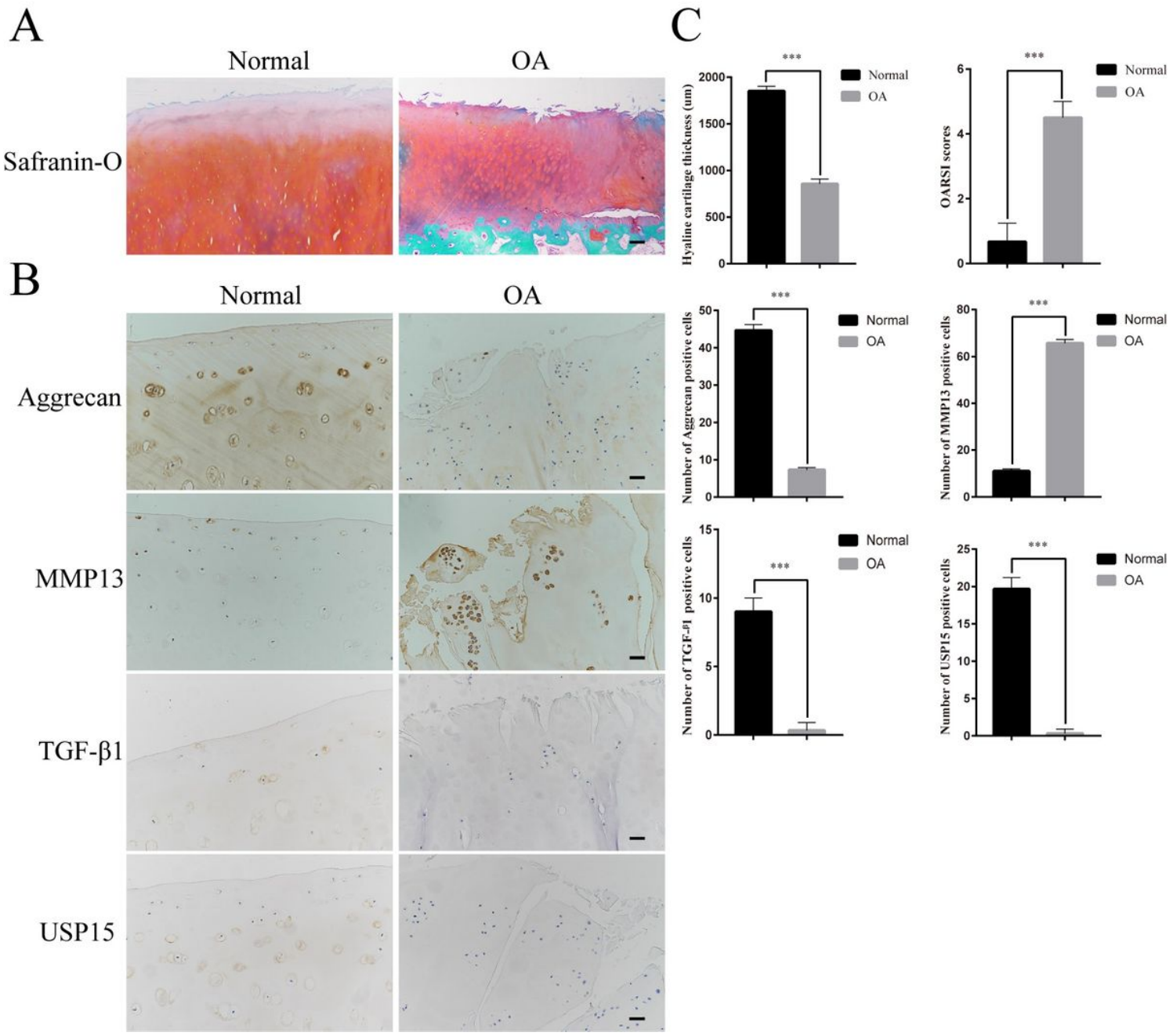

Figure 1

USP15 is negatively correlated with cartilage destruction in human cartilage of OA. (A)The cartilage tissue morphology in the normal and OA human cartilage tissue were detected by Safranin-O fast green staining.(Scale bars=200um).(B) The expression levels of Aggrecan, MMP13, TGF-β1 and USP15 in the normal and OA human cartilage tissue were detected by immunohistochemistry. (Scale bars=50um). (C)The positive cells number of immunohistochemistry ofAggrecan, MMP13, TGF-β1 and USP15in each group were calculated, and the hyaline cartilage thickness and histological analysis of OARSI scores were quantified. The data were presented as the mean ± SD. (*P<0.05, **P<0.01, ***P<0.001).All experiments were performed at least three times.

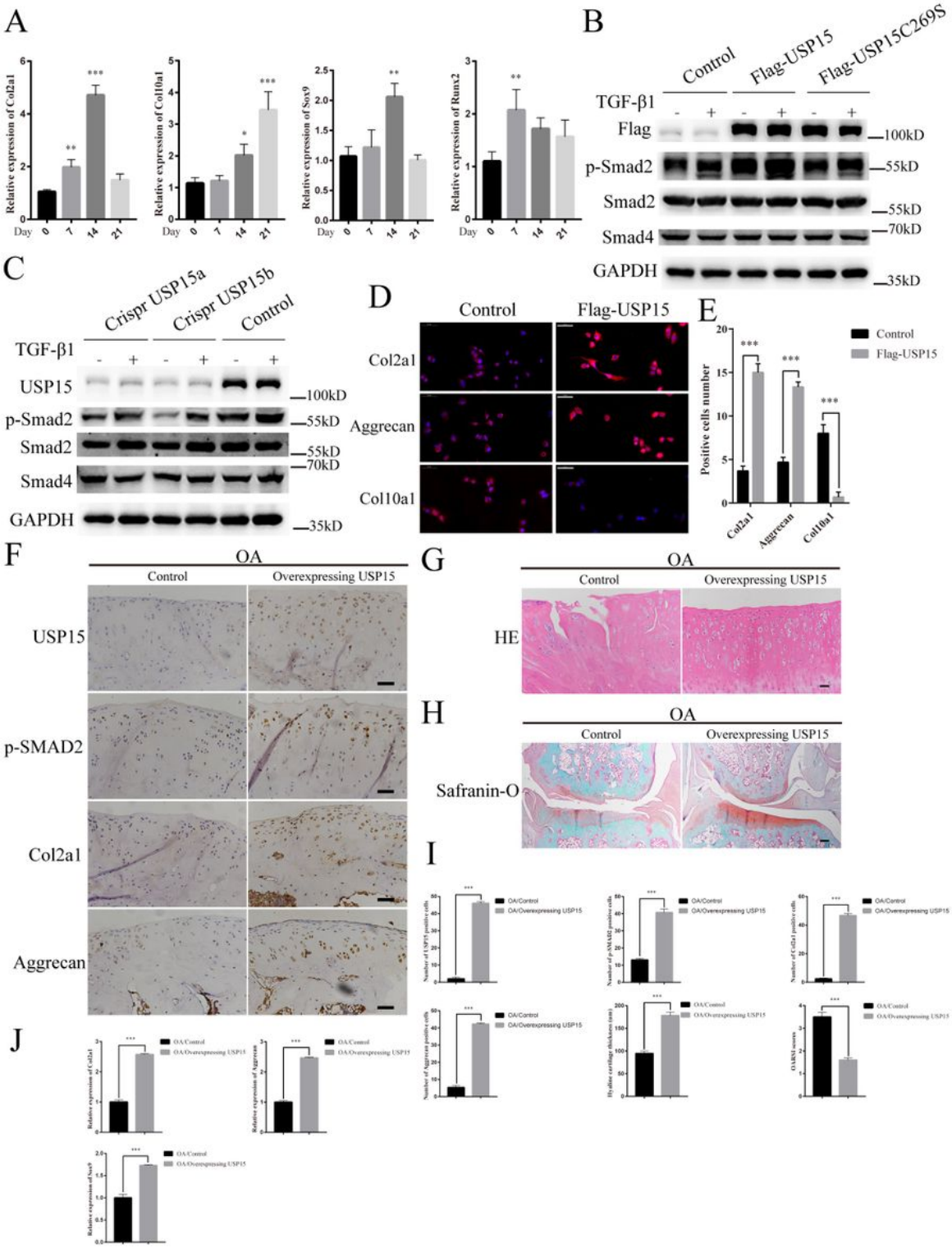

Figure 2

USP15 was conducive to cartilage repair in vivo and in vitro. (A) ITS induction solution was added to induce cartilage phenotype in ATDC5 cells at 7, 14 and 21 days respectively, and real-time quantitative PCR detection of cartilage phenotype related marker molecules was performed. (B-C) Overexpressing or knocking out USP15 in ATDC5 cells with TGF-β1 (10 ng/ml). (D) Immunofluorescence staining performed in ATDC5 cells with or without overexpressing USP15 for Col2a1, Aggrecan and Col10a1. (Scale

bars=50um). (E) The intensity of immunofluorescence of Col2a1, Aggrecan and Col10a1 in each group were calculated, and the data were presented as the mean ± SD. (*P<0.05, **P<0.01, ***P<0.001). (F-H) The expression levels of USP15, p-SMAD2,Col2a1 and Aggrecanin the two groups were detected by immunohistochemistry, and the cartilage tissue morphology in the two groups were detected by HE/Safranin-O fast green staining. (n=4 for control groups in the OA models, n=4 for AAV-mediated USP15 overexpression groups in the OA models). F: (Scale bars=50um). G: (Scale bars=50um). H:(Scale bars=200um). (I) The positive cells number of immunohistochemistry of USP15, p-SMAD2, Col2a1 and Aggrecan in each group were calculated, and the hyaline cartilage thickness and histological analysis of OARSI scores were quantified. The data were presented as the mean ± SD. (*P<0.05, **P<0.01, ***P<0.001). (J) Relative gene expressions of Col2a1, Aggrecan and Sox9 associated with cartilage anabolic metabolism in both groups were detected by real-time quantitative PCR. (n=3 for control groups in the OA models followed by real-time quantitative PCR, n=3 for AAV-mediated USP15 overexpression groups in the OA models followed by real-time quantitative PCR). The data were presented as the mean ± SD. (*P<0.05, **P<0.01, ***P<0.001). All experiments were performed at least three times.

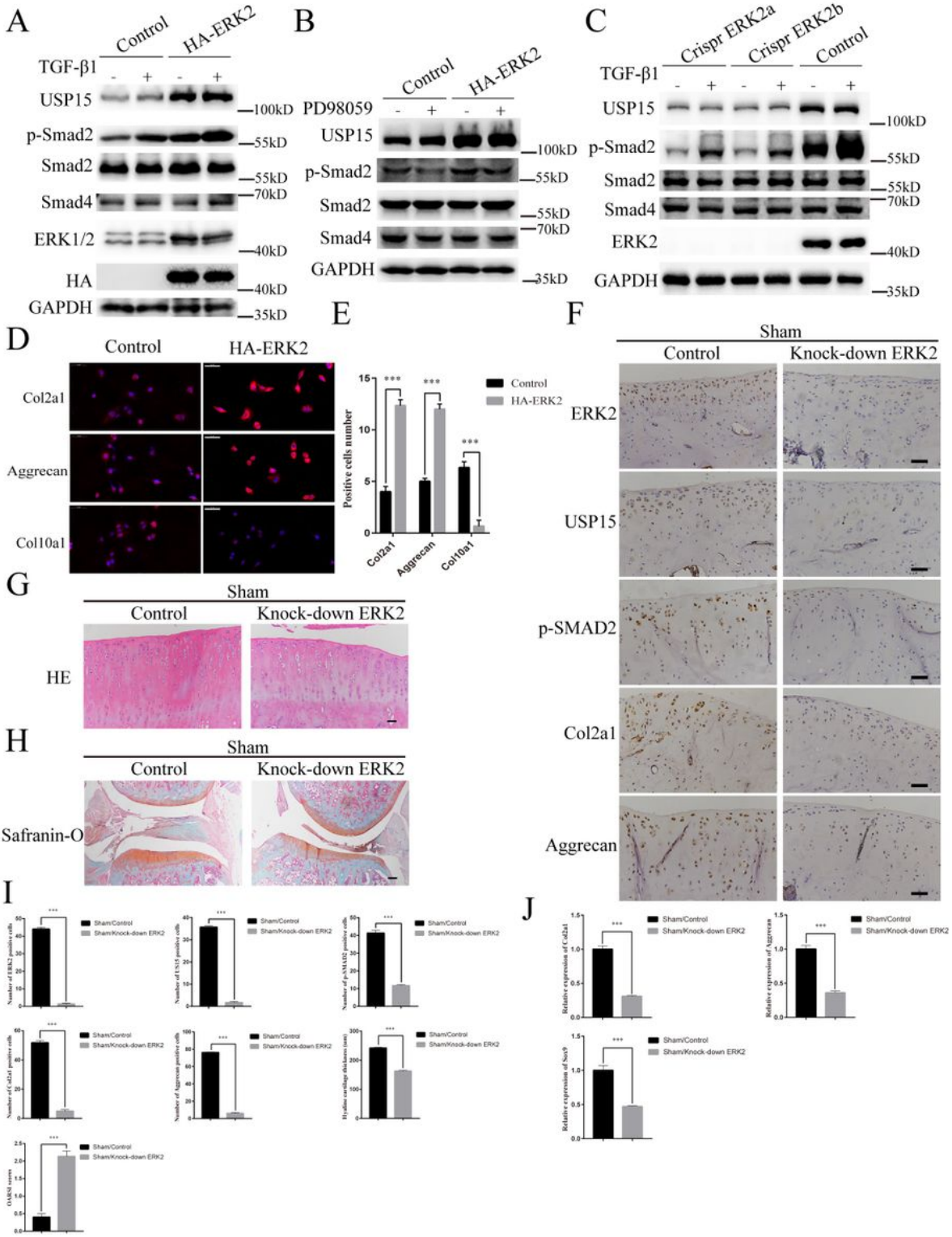

Figure 3

ERK2 can maintain the cartilage phenotype by regulating the TGF-β signaling pathway through USP15. (A-C) Overexpressing or knocking out ERK2 in ATDC5 cells with TGF-β1 (10 ng/ml) or PD98059 (10uM). (D) Immunofluorescence staining performed in ATDC5 cells with or without overexpressing ERK2 for Col2a1, Aggrecan and Col10a1. (Scale bars=50um). (E) The intensity of immunofluorescence of Col2a1, Aggrecan and Col10a1 in each group were calculated, and the data were presented as the mean ± SD.

(*P<0.05, **P<0.01, ***P<0.001). (F-H) The expression levels of ERK2, USP15 and p-SMAD2, Col2a1 and Aggrecanin the two groups were detected by immunohistochemistry, and the cartilage tissue morphology in the two groups were detected by HE/Safranin-O fast green staining. (n=4 for control groups in the sham surgery models, n=4 for AAV-mediated ERK2 knock-down groups in the sham surgery models). F: (Scale bars=50um). G: (Scale bars=50um). H:(Scale bars=200um). (I)The positive cells number of immunohistochemistry of ERK2, USP15, p-SMAD2, Col2a1 and Aggrecan in each group were calculated, and the hyaline cartilage thickness and histological analysis of OARSI scores were quantified. The data were presented as the mean ± SD. (*P<0.05, **P<0.01, ***P<0.001). (J) Relative gene expressions of Col2a1, Aggrecan and Sox9 associated with cartilage anabolic metabolism in both groups were detected by real-time quantitative PCR. (n=3 for control groups in the sham surgery models followed by real-time quantitative PCR, n=3 for AAV-mediated ERK2 knock-down groups in the sham surgery models followed by real-time quantitative PCR). The data were presented as the mean ± SD. (*P<0.05, **P<0.01, ***P<0.001). All experiments were performed at least three times.

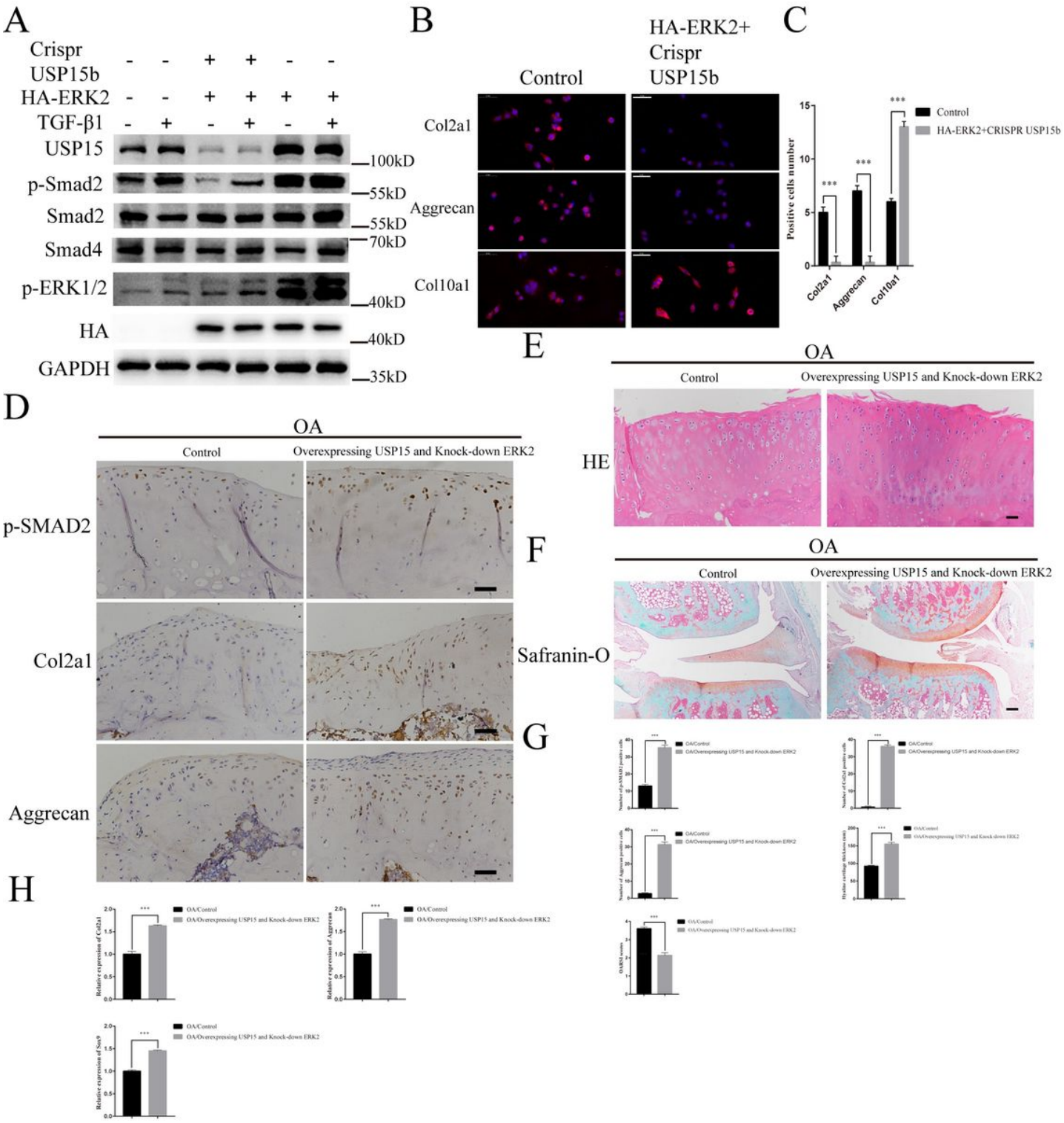

Figure 4

USP15 was required for ERK2 to influence the TGF-β signaling pathway. (A) Overexpressing ERK2 and knocking out USP15 at the same time in ATDC5 cells with TGF-β1 (10 ng/ml). (B) Immunofluorescence staining performed in ATDC5 cells with or without overexpressing ERK2 for Col2a1, Aggrecan and Col10a1. (Scale bars=50um). (C) The intensity of immunofluorescence of Col2a1, Aggrecan and Col10a1 in each group were calculated, and the data were presented as the mean ± SD. (*P<0.05, **P<0.01, ***P<0.001). (D-F) The expression levels of p-SMAD2, Col2a1 and Aggrecanin the two groups were

detected by immunohistochemistry, and the cartilage tissue morphology in the two groups were detected by HE/Safranin-O fast green staining. (n=4 for control groups in the OA models, n=4 for AAV-mediated USP15 overexpression and ERK2 knock-down groups in the OA models). D: (Scale bars=50um). E: (Scale bars=50um). F:(Scale bars=200um). (G) The positive cells number of immunohistochemistry of p-SMAD2, Col2a1 and Aggrecan in each group were calculated, and the hyaline cartilage thickness and histological analysis of OARSI scores were quantified. The data were presented as the mean ± SD. (*P<0.05, **P<0.01, ***P<0.001). (H). Relative gene expressions of Col2a1, Aggrecan and Sox9 associated with cartilage anabolic metabolism in two groups were detected by real-time quantitative PCR. (n=3 for control groups in the OA models followed by real-time quantitative PCR, n=3 for AAV-mediated USP15 overexpression and ERK2 knock-down groups in the OA models followed by real-time quantitative PCR). The data were presented as the mean ± SD. (*P<0.05, **P<0.01, ***P<0.001). All experiments were performed at least three times.

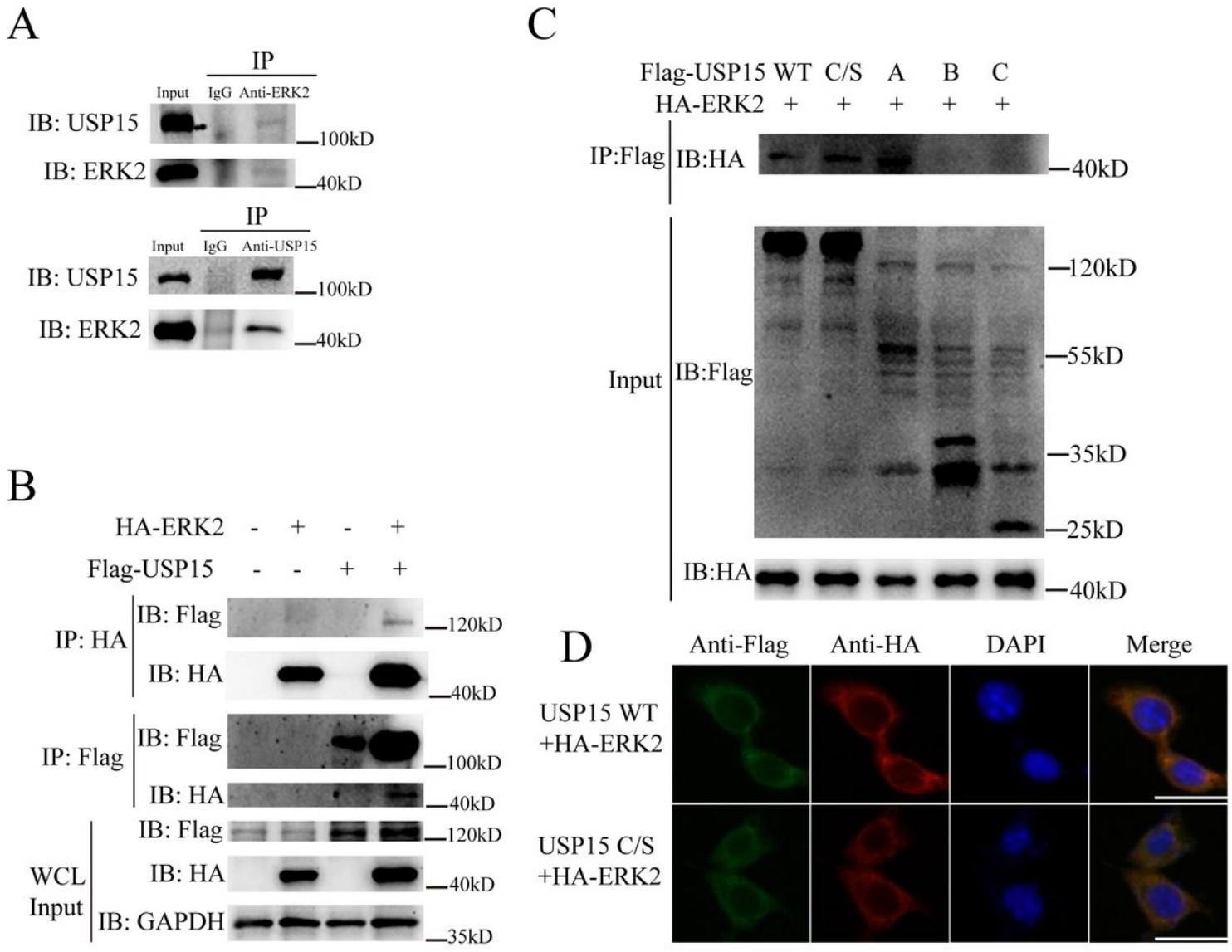

Figure 5

USP15 can form a complex with ERK2. (A) Rat articular chondrocytes were co-immunoprecipitated and examined with the indicated antibodies. (Top) Co-immunoprecipitationwith anti-ERK2 antibodies and immunoblotting with anti-ERK2 or USP15 antibodies, respectively. (Bottom) Co-immunoprecipitationwith anti-USP15 antibodies and immunoblotting with anti-USP15 or ERK2 antibodies, respectively. IgG IP is a negative control. (B) 293T cells were co-transfected with the indicated plasmids, and cell lysates were co-immunoprecipitated with the indicated antibodies and immunoblotted with anti-Flag or anti-HA antibody. (C) 293T cells were co-transfected with HA-ERK2 and Flag-tagged USP15 full-length or its deletion mutants. They were immunoprecipitated with HA antibody and Protein A/G PLUS-Agarose, then immunoblotted with HA and Flag antibodies. A=1-488, B=489-724, C=725-952. (D) Immunofluorescent detection of Flag-USP15, Flag-USP15C269S, and HA-ERK2 in ATDC5 cells. Nuclei are counterstained by DAPI.Scale bars=50um.

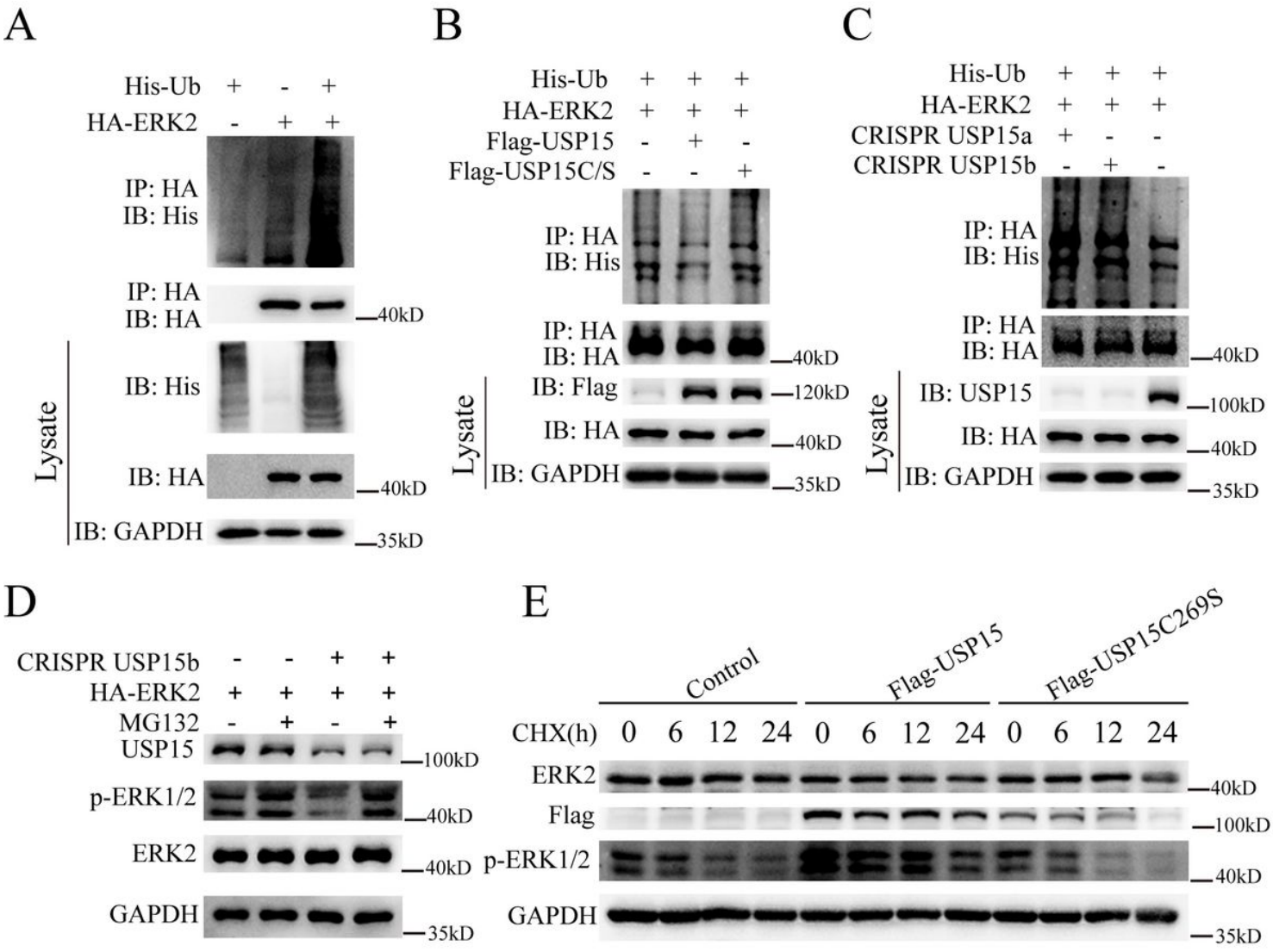

Figure 6

USP15 regulated the ubiquitination of ERK2. (A) ATDC5 cells were infected with stable co-lentiviral vectors HA-ERK2 and His-Ubiquitin (Ub) and immunoprecipitated with HA antibody and Protein A/G PLUS-Agarose, and then immunoblotted with antibodies against HA and His. (B) ATDC5 cells were

infected with stable co-lentiviral vectors HA-ERK2, His-Ubiquitin (Ub), Flag-USP15 and Flag-USP15C269S. They were immunoprecipitated with HA antibody and Protein A/G PLUS-Agarose, and then immunoblotted with antibodies against HA and His. (C) ATDC5 cells were infected with stable co-lentiviral vectors HA-ERK2, His-Ubiquitin (Ub), Crispr USP15a and Crispr USP15b. They were co-immunoprecipitated with HA antibody and Protein A/G PLUS-Agarose, and then immunoblotted with antibodies against HA and His. (D) Immunoblot analysis of ATDC5 cells overexpressing ERK2 and Crispr USP15b in the presence or absence of MG132 (5uM) treatment. (E) ATDC5 cells were infected with stable lentiviral vectors Flag-USP15 and Flag-USP15C269S and treated with cycloheximide (100 μg/ml). Immunoblotting was performed with the indicated antibodies and collected at the indicated times.

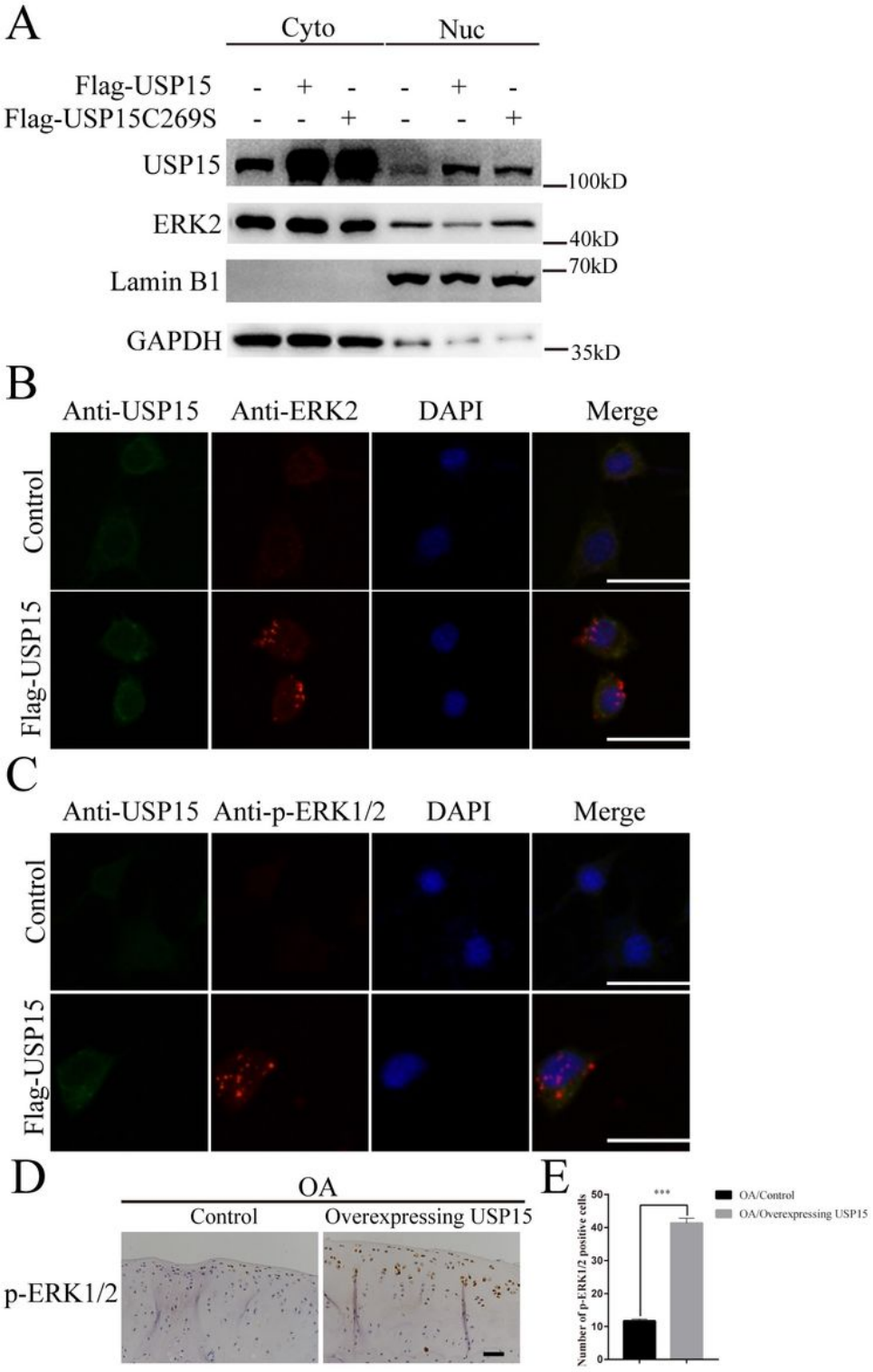

Figure 7

USP15 changed the location of ERK2 and stimulates the amount of phosphorylated ERK2. (A) ATDC5 cells infected with co-lentiviral vectors Flag-USP15 and Flag-USP15C269S were collected for cytoplasm and nuclear extraction, followed by immunoblot analysis. (B-C) Immunofluorescence and DAPI staining of ATDC5 cells infected with stable lentiviral vectors Flag-USP15 and then detected by USP15, ERK2 and p-ERK1/2 antibodies. Scale bars=50um. (D) The expression levels of p-ERK1/2 in the two groups were

detected by immunohistochemistry. (n=4 for control groups in the OA models, n=4 for AAV-mediated USP15 overexpression groups in the OA models). D: (Scale bars=50um). (E) The positive cells number of immunohistochemistry of p-ERK1/2 in each group were calculated. The data were presented as the mean ± SD. (*P<0.05, **P<0.01, ***P<0.001).

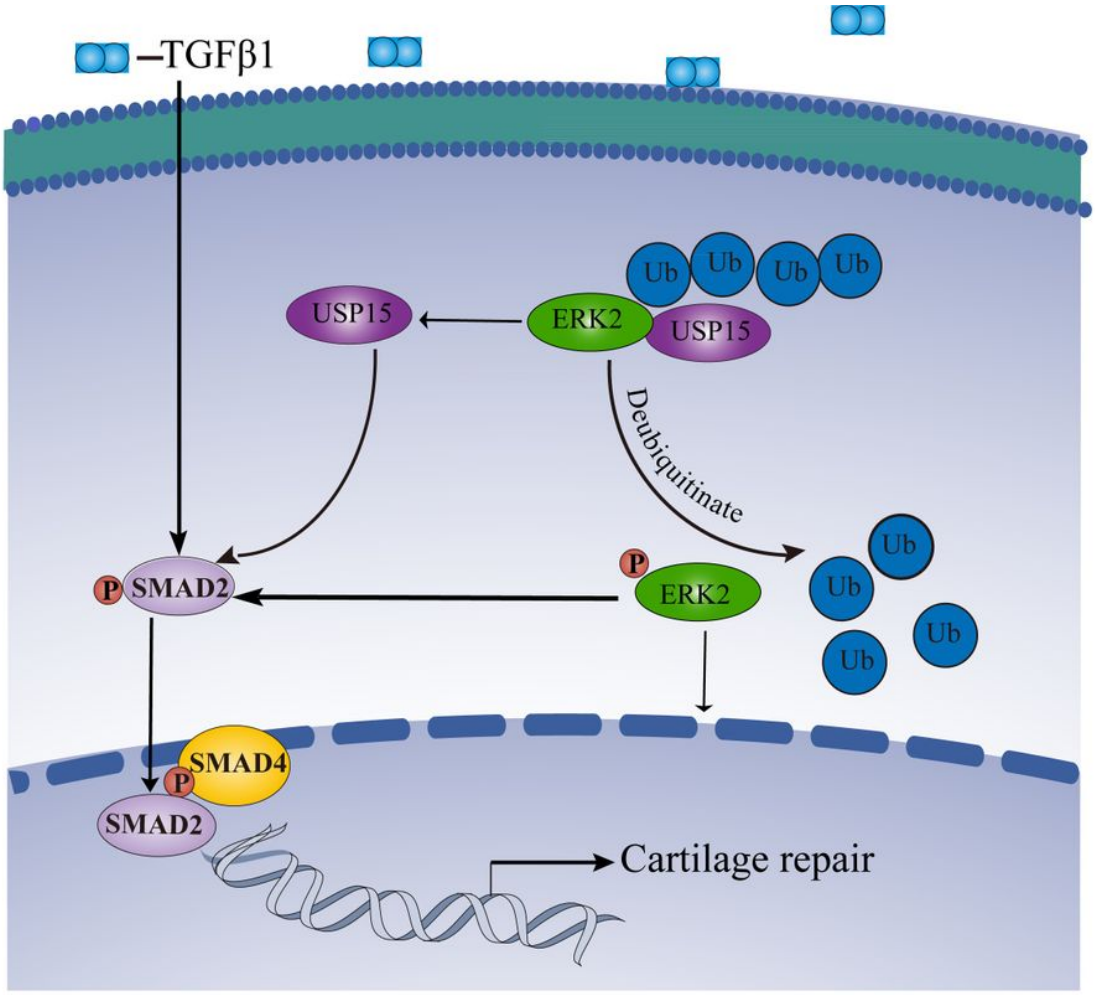

Figure 8

A working model for positive feedback regulation between USP15 and ERK2 playing a critical role in osteoarthritis. Non-SMAD of ERK2 can increase the levels of USP15 and activate p-SMAD2. Then USP15 can interact with and deubiquitinate ERK2. Next, ERK2 can be activated by USP15, and phosphorylated ERK2 from the cytoplasm is translocated to the nucleus. Finally, this positive feedback loop can increase levels of the cartilage repair markers.

Supplementary Files

This is a list of supplementary files associated with this preprint. Click to download.

- Supplementfigure1.tif
- Supplement.docx